The Development of Two Composite Energy Absorbers for Use in a Transport Rotorcraft Airframe Crash Testbed (TRACT 2) Full-Scale Crash Test

Justin D. Littell
NASA Langley Research Center

Karen E. Jackson
NASA Langley Research Center

Martin S. Annett
NASA Langley Research Center

Michael D. Seal
Analytical Mechanics Associates, Inc.

Edwin L. Fasanella
National Institute of Aerospace

NASA Langley Research Center
Hampton, VA 23681

ABSTRACT

Two composite energy absorbers were developed and evaluated at NASA Langley Research Center through multi-level testing and simulation performed under the Transport Rotorcraft Airframe Crash Testbed (TRACT) research program. A conical-shaped energy absorber, designated the conusoid, was evaluated that consisted of four layers of hybrid carbon-Kevlar® plain weave fabric oriented at [+45°/-45°/-45°/+45°] with respect to the vertical direction. A sinusoidal-shaped energy absorber, designated the sinusoid, was developed that consisted of hybrid carbon-Kevlar® plain weave fabric face sheets, two layers for each face sheet oriented at ±45° with respect to the vertical direction, and a closed-cell ELFOAM® P200 polyisocyanurate (2.0-lb/ft^3) foam core. The design goal for the energy absorbers was to achieve average floor-level accelerations of between 25- and 40-g during the full-scale crash test of a retrofitted CH-46E helicopter airframe, designated TRACT 2. Variations in both designs were assessed through dynamic crush testing of component specimens. Once the designs were finalized, subfloor beams of each configuration were fabricated and retrofitted into a barrel section of a CH-46E helicopter. A vertical drop test of the barrel section was conducted onto concrete to evaluate the performance of the energy absorbers prior to retrofit into TRACT 2. The retrofitted airframe was crash tested under combined forward and vertical velocity conditions onto soft soil. Finite element models were developed of all test articles and simulations were performed using LS-DYNA®, a commercial nonlinear explicit transient dynamic finite element code. Test-analysis results are presented for each energy absorber as comparisons of time-history responses, as well as predicted and experimental structural deformations and progressive damage under impact loading for each evaluation level.

INTRODUCTION

In 2012, the NASA Rotary Wing (RW) Crashworthiness Program [1] initiated the Transport Rotorcraft Airframe Crash Testbed (TRACT) research program by obtaining two CH-46E helicopter airframes from the Navy CH-46E Program Office (PMA-226) at the Navy Flight Readiness Center in Cherry Point, North Carolina. Full-scale crash tests were planned to assess dynamic responses of transport-category rotorcraft under combined forward and vertical impact loading. The first crash test, TRACT 1 [2], was performed at NASA Langley Research Center's Landing and Impact Research Facility (LandIR), which enables the study of critical interactions between the airframe, seat, and occupant during a controlled crash environment. The CH-46E fuselage is categorized as a medium-lift rotorcraft with length and width of 45- and 7-ft, respectively, and a capacity for 5 crew and 25 troops. TRACT 1 was conducted in August 2013 under combined conditions of 300-in/s (25-ft/s) vertical and 396-in/s (33-ft/s)

Presented at the AHS 71st Annual Forum, Virginia Beach, Virginia, May 5–7, 2015.

forward velocity onto soil, which is characterized as a sand/clay mixture. The primary objectives for TRACT 1 were to assess improvements in occupant loads and flail envelope with the use of crashworthy features such as pre-tensioning active restraints and energy absorbing seats and to develop novel techniques for photogrammetric data acquisition to measure occupant and airframe kinematics. A post-test photograph of the TRACT 1 crash test is shown in Figure 1.

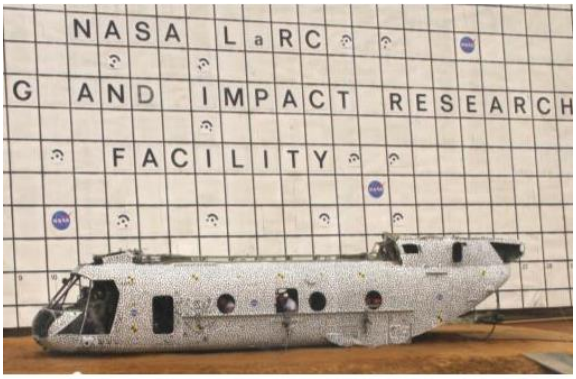

Figure 1. Post-test photographs of the TRACT 1 full-scale crash test.

The TRACT 1 airframe was tested in a baseline configuration with no changes to the structural configuration, including the discrete aluminum shear panels in the subfloor. It is important to note that the CH-46E does not contain a center keel beam, and, thus, relies on the aluminum shear panels, the cargo rails in the floor, and the airframe structure to provide longitudinal and torsional stiffness. A final objective of TRACT 1 was to generate crash test data in a baseline configuration for comparison with data obtained from a similar TRACT 2 crash test. The crash test of the second CH-46E airframe (TRACT 2) was conducted on October 1, 2014 and was performed for the same nominal impact velocity conditions and the same impact surface [3]. The difference is that the TRACT 2 airframe was retrofitted with three different composite energy absorbing subfloor concepts: a corrugated web design [4, 5] fabricated of graphite fabric; a conical-shaped design, designated the "conusoid," fabricated of four layers of hybrid carbon-Kevlar® fabric [6]; and, a sinusoidal-shaped foam sandwich design, designated the "sinusoid," fabricated of the same hybrid fabric face sheets with a foam core. This paper will discuss the results of the conusoid and sinusoid only. The corrugated web design is presented in [4,5]. While the TRACT 2 airframe contained similar seat, occupant, and restraint experiments, one of the major goals of the test was to evaluate the performance of novel composite energy absorbing subfloor designs for improved crashworthiness.

This paper will summarize the development of the conusoid and sinusoid foam sandwich energy absorbing concepts. Multi-level evaluations of the energy absorbers are discussed including dynamic crush testing and simulation of component specimens, vertical drop testing and simulation of a retrofitted barrel section, and full-scale crash testing and simulation of the TRACT 2 retrofitted helicopter airframe. Finite element models were developed of all test articles and simulations were performed using LS-DYNA® [7, 8], a commercial explicit nonlinear, transient dynamic finite element code. Thus, a final objective of this research program is to evaluate the capabilities of LS-DYNA® simulations in predicting the dynamic response and progressive failure behavior of composite energy absorbing airframe structures.

COMPOSITE ENERGY ABSORBING CONCEPTS

Following the TRACT 1 crash test, a research effort was initiated to develop two composite energy absorbers for retrofit into the TRACT 2 test article. The design goals were to achieve between 25- to 40-g sustained average crush accelerations, to minimize peak crush loads, and to generate relatively long crush stroke limits under dynamic loading conditions, typical of those experienced during the TRACT 1 full-scale crash test.

Conusoid Energy Absorber

First of the two energy absorbing concepts was a sinusoid shaped beam made up of conical half sections, colloquially named the "conusoid". The geometry of the conusoid is based on alternating right-side-up and up-side down half-cones placed in a repeating pattern. The conusoid combines a simple cone design, which has been extensively studied in the literature [9-12], with sinusoidal beam geometry to create a structure that utilizes the advantages of both configurations.

Variations in geometry, materials, and laminate stacking sequences were evaluated during development of the conusoid and the final design consisted of four layers of a hybrid carbon-Kevlar® plain weave fabric oriented at [+45°/-45°/-45°/+45°] with respect to the vertical direction. A photograph of

a typical conusoid component is shown in Figure 2. Dimensions of the component are 12-in. long, 7.5-in. to 9-in. high, with an overall width of 1.5-in. Additional information on the development and fabrication of the conusoid energy absorber may be found in Reference 6.

Figure 2. Conusoid Component.

Sinusoid Foam Sandwich Energy Absorber

The second energy absorber, designated the "sinusoid," consisted of hybrid carbon-Kevlar® plain weave fabric face sheets, two layers for each face sheet oriented at ±45° with respect to the vertical direction, and a closed-cell ELFOAM® P200 polyisocyanurate (2.0-lb/ft^3) closed-cell foam core. Sine wave energy absorbers have been studied extensively because they offer desirable features under compressive loading [13-17]. Energy absorption values from sine wave concepts can be similar to values obtained from crush tubes. In addition, sine wave concepts tend to deform in a stable manner through plastic hinge formation and crushing, rather than global buckling. However, it should be noted that the sinusoid concept described in this paper is not a true sinusoidal shape, but actually a series of half circles; however, the designation of "sinusoid" will continue to be used. A sinusoid component with top and bottom face sheets used in testing is shown in Figure 3.

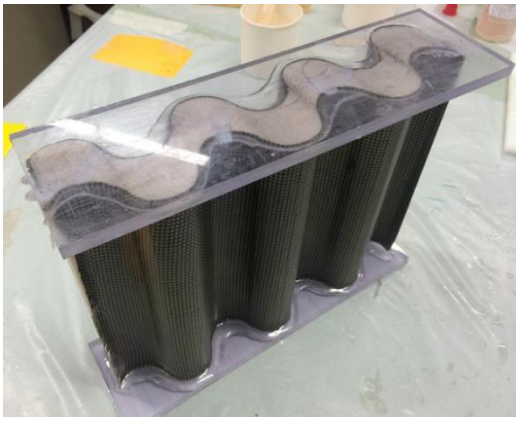

Figure 3. Sinusoid Component.

COMPONENT TESTING AND SIMULATION

Component Dynamic Crush Testing

Representative component specimens for both the conusoid and the sinusoid were manufactured in-house at NASA LaRC, and are shown in Figures 2 and 3. Each specimen was approximately 1-ft. in linear length and approximately 7.5 to 9-in tall, depending on needed amount of edge trimming. The specimens were potted into clear polycarbonate sheets to facilitate testing. The two energy absorbers were dynamically crushed in a 14-ft. drop tower with an instrumented 110-lb. falling mass. The impact condition for all of the dynamically crushed specimens was approximately 264-in/s (22-ft/s). The drop mass was instrumented with a 500-g damped accelerometer and data were acquired using a National Instruments Data Acquisition System (DAS) sampling at 25-kHz. All post-processed acceleration data were filtered using a low-pass 4-pole Butterworth filter with a 500-Hz cutoff frequency. A high-speed camera filming at 1-kHz captured the deformation time history. An example test sequence of the conusoid component crush test is depicted in Figure 4. The identified failure mechanism is folding of the conusoid walls, which is a desirable failure mode that produces a stable and constant crush response within the design level of 25-40 g. Similar data were obtained from the sinusoid specimen.

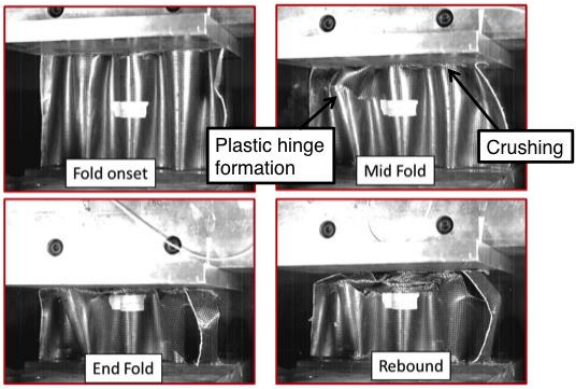

Figure 4. High-speed video clips of conusoid deformation.

Component Dynamic Crush Simulations

Finite element models were created to represent both the conusoid and sinusoid component level specimens. A depiction of the finite element model representing the conusoid energy absorber is shown in Figure 5.

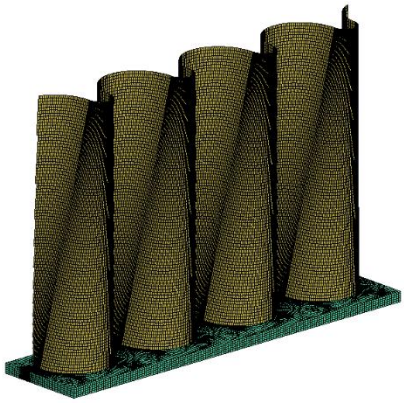

Figure 5. The conusoid component model.

The conusoid component model contained 185,940 nodes; 44,294 Belytschko-Tsay shell elements; 116,100 solid elements representing the rigid drop mass, 1 initial velocity card assigned to nodes forming the rigid mass (not shown in Figure 5), and 1 body load card defining gravity. The nominal shell element edge length is 0.032-in. The shell elements representing the hybrid carbon-Kevlar® fabric layers were assigned Mat 58, which is a continuum damage mechanics material model used in LS-DYNA® for representing composite laminates and fabrics [18].

Baseline Mat 58 properties are listed in Table 1. Properties for Mat 58 were obtained through detailed test-analysis comparisons with experimental data obtained from standard material characterization tests, such as tensile testing of fabric coupons oriented at 0°, 90°, and ±45° to obtain longitudinal stiffness and strength, transverse stiffness and strength, and shear stiffness and strength, respectively. Once verified through comparison with coupon test data, these properties were unchanged for all subsequent simulations of the energy absorbers. It should be noted that Mat 58 includes certain parameters, such as the SLIM parameters and ERODS that cannot be determined entirely based on experimental data. For these parameters, estimates were input based on past experience of the analysts. For the conusoid, individual ply layers were input using the *PART_COMPOSITE feature in LS-DYNA® which allows input of ply orientations, ply thicknesses, and ply material designations for each layer within a composite laminate. Single Point Constraints (SPCs) were used to constrain the nodes forming the bottom plate.

Table 1. Mat 58 Material properties used to represent carbon-Kevlar® fabric.

Material Property Description	Symbol	Values
Density, lb-s^2/in^4	RO	1.29E-4
Young's modulus longitudinal direction, psi	EA	6.3E+6
Young's modulus transverse direction, psi	EB	2.76E+6
Poisson's ratio, ν_{21}	PRBA	0.03
Stress limit of nonlinear portion of shear curve, psi	TAU1	4,500.
Strain limit of nonlinear portion of shear curve, in/in	GAMMA1	0.06
Shear modulus AB, BC, and CA, psi	GAB	3.0E+5
Min stress factor for limit after max stress (fiber tension)	SLIMT1	0.8
Min stress factor for limit after max stress (fiber comp)	SLIMC1	1.0
Min stress factor for limit after max stress (matrix tension)	SLIMT2	0.8
Min stress factor for limit after max stress (matrix comp)	SLIMC2	1.0
Min stress factor for limit after max stress (shear)	SLIMS	1.0

Material axes option (model dependent)	AOPT	0.0
Maximum effective strain for element layer failure	ERODS	0.5
Failure surface type	FS	-1.0
Strain at longitudinal compressive strength, in/in	E11C	0.007
Strain at longitudinal tensile strength, in/in	E11T	0.0143
Strain at transverse compressive strength, in/in	E22C	0.012
Strain at transverse tensile strength, in/in	E22T	0.025
Strain at shear strength, in/in	GMS	0.45
Longitudinal compressive strength, psi	XC	40,000.
Longitudinal tensile strength, psi	XT	89,000.
Transverse compressive strength, psi	YC	25,000.
Transverse tensile strength, psi	YT	54,000.
Shear strength, psi	SC	7,100.

The sinusoid component model contained: 53,540 nodes; 7,380 Belytschko-Tsay shell elements; 37,515 solid elements; a rigid drop mass; 1 initial velocity card assigned to nodes forming the rigid drop mass; SPCs to fully constrain the bottom nodes of the sinusoid; 1 automatic single surface contact; and 3 material definitions. As with the conusoid, the shell elements were assigned Mat 58, using the properties listed in Table 1. The nominal element edge length in the sinusoid model was 0.2-inches.

The solid elements representing the foam core were assigned Mat 63, which is a crushable foam material model in LS-DYNA® that allows user input of the stress-strain response of the material in tabular format. The stress-strain response of the P200 foam was determined through quasi-static testing of 4-in. x 4-in. x 3-in. rectangular blocks. A plot of the experimental curve obtained at a crush rate of 1.0-in/minute is shown in Figure 6, along with the stress-strain response used as input to Mat 63. Note that the input curve matches the test data to a strain of 0.67-in/in. At this point, the test data ends, yet the Mat 63 input response continues and increases dramatically up to 100,000-psi at 1-in/in (note that this data point is not shown in the plot). The large "tail" added to the end of the stress-strain response represents compaction of the foam and is needed to stabilize the response of the solid elements for high values of volumetric strain.

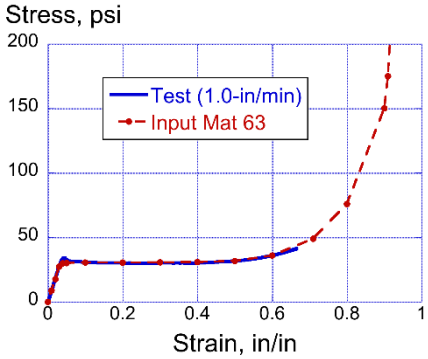

Figure 6. Stress strain response for the P200 foam core

A depiction of the finite element model representing the sinusoid energy absorber component is shown in Figure 7.

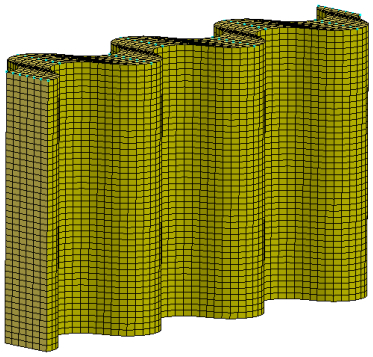

Figure 7. The sinusoid component model.

Comparisons of predicted and experimental acceleration and displacement time histories of the drop mass from the conusoid impact tests are shown in Figures 8(a) and (b), respectively. The conusoid model over predicts the magnitude of the initial peak acceleration, 96-g compared with 61-g for the test. However, other than that anomaly, the level of agreement is good. The average acceleration calculated for the test is 28.0-g for pulse duration of 0.0- to 0.025-s, whereas the model average acceleration is 28.4-g for the same duration. The results of the conusoid component test indicate that the configuration of the energy absorber meets all of the design goals, including achieving a sustained acceleration level of between 25-40-g. The comparison of vertical displacement time histories also exhibits good agreement, as shown in Figure 6(b). The maximum displacement of the test article is 2.9-

in., providing a crush stroke of 38.7%. The maximum displacement of the model is 2.53-in., providing a crush stroke of 33.7%.

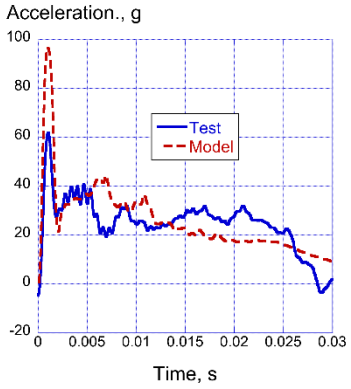

(a) Acceleration responses

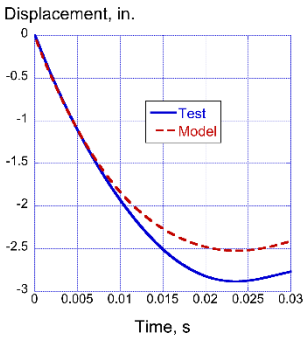

(b) Displacement responses.

Figure 8. Acceleration and displacement comparisons for the conusoid component.

Test-analysis comparisons of time-history responses are plotted in Figure 9(a) and (b) for the sinusoid component crush test. These results demonstrate excellent test-analysis agreement. As can be seen in Figure 9(a), the acceleration response of the drop mass achieves an initial peak of 55-g, then drops to approximately 22-g, where it remains constant until the end of the pulse. The model mimics this response, even predicting the unloading response near the end of the pulse. The average acceleration calculated for the test is 21.8-g for pulse duration of 0.0- to 0.03-s, whereas the average acceleration of the predicted response is 22.9-g for the same duration. The experimental and analytical displacement responses, shown in Figure 9(b), exhibit maximum values of 4- and 3.8-in., respectively, which represents approximately 50% stroke. The average acceleration results for the sinusoid fall slightly below the required design goal of 25- to 40-g. The lower average crush acceleration for the sinusoid translates into a larger crush stroke than was seen for the conusoid.

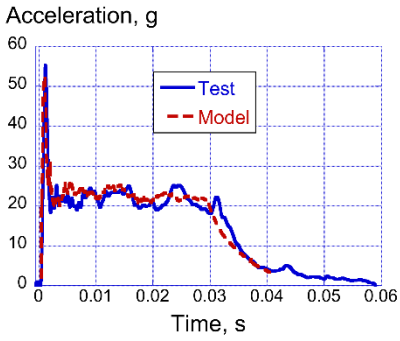

(a) Acceleration responses

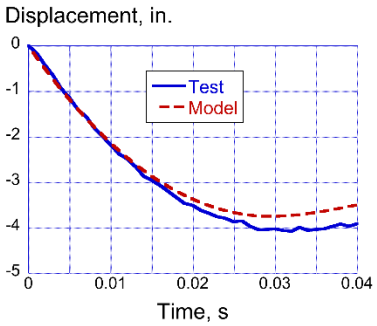

(b) Displacement responses.

Figure 9. Test-analysis time history comparisons for the sinusoid component.

RETROFITTED BARREL SECTION DROP TESTING AND SIMULATION

Barrel Section Test Article

Following an extensive investigation into the properties of the sinusoid and conusoid component energy absorbers, a full scale drop test was proposed to further their development and understanding. An undamaged portion of the forward cabin section (Fuselage Station FS164 through FS250) was removed from the tested TRACT 1 airframe for use as the drop test article to evaluate the energy absorbing concepts prior to the full scale TRACT 2 crash test. Figure 10 shows the removed barrel section used for the drop test.

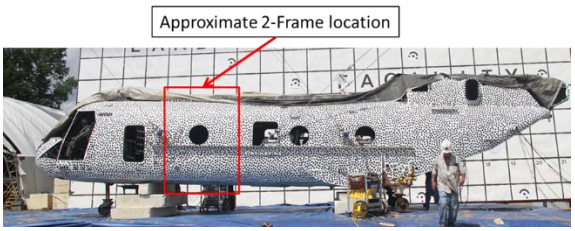

Figure 10. 2-Frame barrel section location removed from TRACT test article

A full scale concept of both the conusoid energy absorber and the sinusoid energy absorber were fabricated and retrofitted into the subfloor frame sections of the barrel section test article. The full scale energy absorbers are shown in Figure 11.

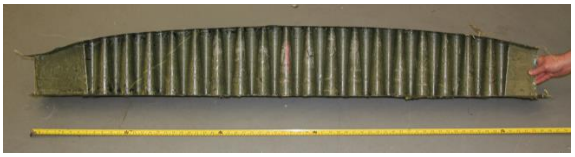

(a) Conusoid energy absorber

(b Sinusoid energy absorber

Figure 11. Full scale energy absorbers used in barrel drop test

The original floor in the barrel section was removed and was replaced with a sheet of 0.5-in.-thick polycarbonate. The reason for this change was to enable viewing of the crushing response of the energy absorbers using high-speed cameras. Ballast, in the form of a seat, 2 ATDs, and a 320-lb. lead weight giving a total weight of 725-lb. was placed above the sinusoid energy absorber, while steel I-beams and lead weights weighing a total of 681-lb.were placed over the conusoid energy absorber. Accelerometers were attached to the lead weights to determine crush acceleration of the energy absorbers.

The total weight of the fully loaded barrel section was 1,810-lb. It was impacted onto concrete at 297.6-in/s (24.8-ft/s). Figure 12 shows photographs of the barrel section test article.

(a) Front view.

(b) Close-up front view of the installed sinusoid

(c) Rear view.

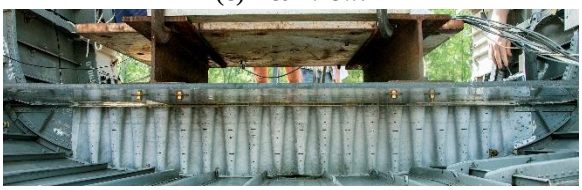

(d) Close-up rear view of the installed conusoid

Figure 12. Front and rear view photographs of the barrel test article.

Barrel Section Model Characteristics

The finite element model of the barrel section is shown in Figure 13. This model contains: 105,986 nodes; 22 parts; 10 material definitions; 57,041 Belytschko-Tsay shell elements; 63,591 solid elements; 1,677 beam elements; 1 initial velocity; 1 contact definition; 20 discrete masses representing the double seat and ATD

occupants; 2 lumped masses representing the 320- and 681-lb blocks used in the test article; and 1 planar rigid wall representing the impact surface, which is not shown in Figure 13. The seat and occupants were represented using 20 discrete masses assigned to nodes at the approximate seat track attachment locations. All nodes in the barrel section model were assigned an initial velocity of 297.6-in/s (24.8-ft/s), matching the measured test velocity. The aluminum outer skin and frames were assigned properties of Mat 24, an elastic-plastic material model. The steel bolts were simulated using beam elements that were assigned material properties of hardened steel.

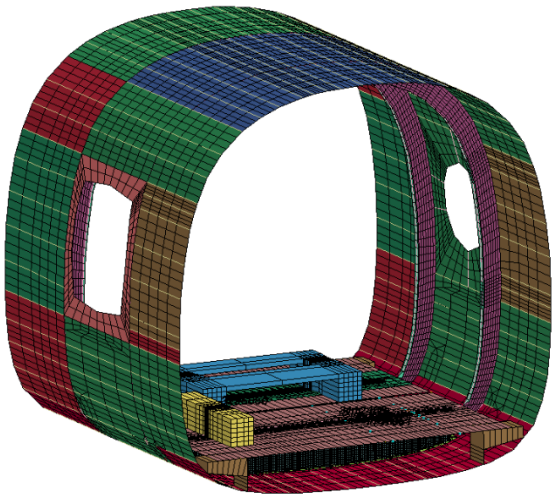

Figure 13. The barrel test article finite element model

The models of the conusoid and sinusoid energy absorber models are shown in Figure 14. The conusoid material model was created using a stackup sequence and materials shown in Table 1, which were developed from the component tests. A nominal element edge length of 0.3-in. was used in the conusoid mesh. Similarly, the sinusoid energy absorber model was developed using materials and geometries created from the component tests. A nominal element edge length of 0.25-in. was used in the sinusoid mesh. Note that in the test article, the energy absorbers were attached to the outer skin and floor using rivets. In the model, the rivets were not physically modeled, however, coincident nodes were used to tie the parts together.

An automatic single surface contact was assigned to the model with static and dynamic coefficients of friction of 0.3. This general contact definition is used to prevent any node from penetrating any element within the model. The model was executed using LS-DYNA® SMP version 971 on a Linux-based workstation with 8 processors and required 31.75 hours of clock time to execute the simulation for 0.065-seconds. Model output included time-history responses of the 320- and 681-lb lumped masses, and image sequences of structural deformation.

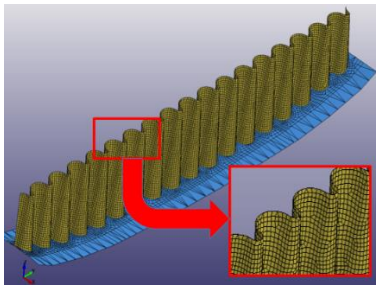

(a) Conusoid energy absorber

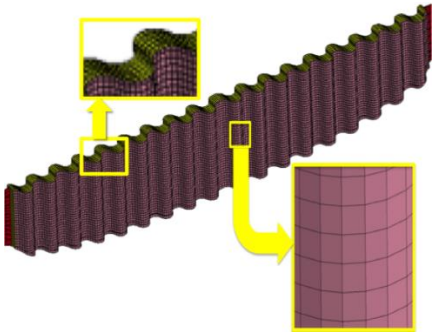

(b) Sinusoid energy absorber

Figure 14. Depictions of the finite element models of the two energy absorbing subfloors retrofitted into the barrel section.

Barrel Section Test-Analysis Comparisons

Test-analysis time history responses of acceleration and velocity of the 681-lb mass, located above the conusoid energy absorber, are plotted in Figure 15. Both the test and predicted acceleration responses exhibit a significant increase in acceleration near the end of their pulses. The test response exhibits a 34.5-g peak at 0.044-s, whereas the model peak of 55.9-g occurs at 0.033-s. Average accelerations of 15.0- and 17.5-g were calculated for the test and predicted responses, respectively, for a pulse duration of 0.0- to 0.06-s. The velocity responses in Figure 15(b) indicate that the model is too stiff and predicted velocity is removed much more quickly than for the test. In addition, the model predicts a much higher rebound velocity than the test, which indicates that the model contains too much elastic energy and that the

unloading response is not adequately captured. The predicted maximum crush displacement is 7.8-in. and the experimental maximum crush displacement is 8.67-in., a difference of approximately 0.9-in. Finally, it should be noted that the average test acceleration response falls well below the design goal of 25- to 40-g.

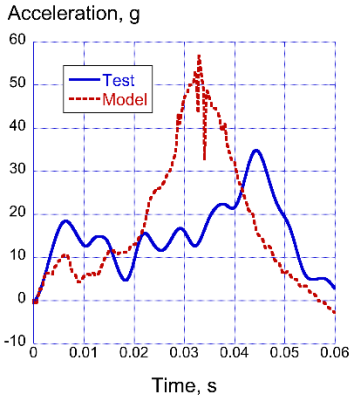

(a) Acceleration of 681-lb mass

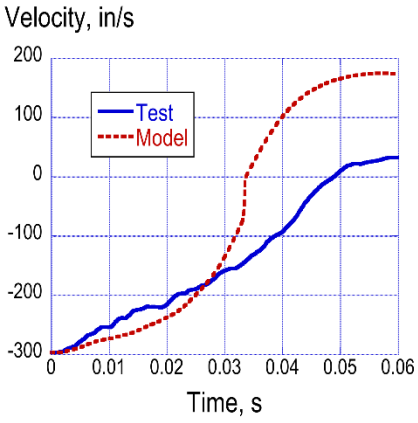

(b) Velocity of 681-lb. mass

Figure 15. Test vs. Analysis response of the 681-lb mass located over the conusoid energy absorber

Figure 16 shows comparisons between the test and analysis for the final deformed shape of the conusoid subfloor. The crush pattern is non-uniform due to the fact that the 681-lb mass is actually attached to the floor using two I-beams separated by 26-in. with flange widths of 6-in. The sides of the conusoid subfloor that attach to the fuselage frames are relatively undamaged. It is also interesting to note the permanent deformation pattern of the polycarbonate floor above the conusoid.

(a) Model deformation of conusoid energy absorber

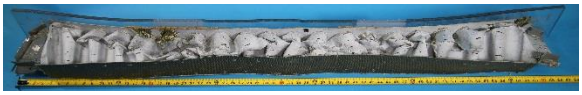

(b) Test deformation of conusoid energy absorber

Figure 16. Test vs Model deformation of the conusoid energy absorber

Test-analysis time-history responses of the 320-lb mass, located above the sinusoid energy absorber, are plotted in Figure 17. While the predicted responses demonstrate reasonable comparison with test, the model fails to predict the large increase in acceleration that occurs just prior to 0.03-s. This 64-g peak is attributed to contact that two steel bolts which were bolting the mass onto the floor, made with the outer skin. Even though the model includes the bolts, the predicted acceleration response does not match the test. Average accelerations of 14.2- and 17.0-g were calculated for the test and predicted responses, respectively, for a pulse duration of 0.0- to 0.0575-s. It should be noted that average test and predicted accelerations are well below the design goal of 25- to 40-g. The test-analysis velocity responses are shown in Figure 17(b), both of which cross zero at the same time (0.0326-s), even though the test and predicted curves deviate shortly after 0.01-s. The model predicts a much higher rebound velocity than the test, which indicates that the model returns too much elastic energy and that the unloading response is not adequately represented. The predicted maximum crush displacement is 5.24-in. and the experimental maximum crush displacement is 6.3-in., a difference of approximately 1-in.

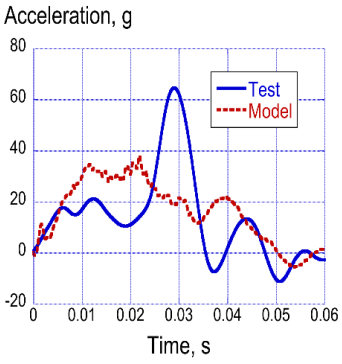

(a) Acceleration of 320-lb mass

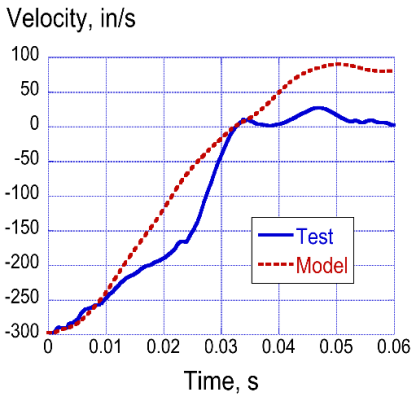

(a) Velocity of 320-lb mass

Figure 17. Test vs. Analysis response of the 320-lb weight located over the sinusoid energy absorber

Figure 18 shows comparisons between the test and analysis for the final deformed shape of sinusoid subfloor. The model shows a much larger permanent crush displacement than what was seen in the test. Also, the test displacement shows a much more uniform crush response than the model

(a) Model deformation of sinusoid energy absorber

(b) Test deformation of sinusoid energy absorber

Figure 18. Test vs Model deformation of the sinusoid energy absorber

The barrel test results showed, in part, that both of the fabricated energy absorbers performed as expected through their progressive crushing and load limiting characteristics. They should be included for evaluation of performance in a full-scale crash test.

TRACT 2 CRASH TEST AND SIMULATION

TRACT 2 Crash Test

A second CH-46E helicopter airframe was prepared for crash testing and loaded in a similar manner as the TRACT 1 test article. In addition, the TRACT 2 aircraft was retrofitted with three different composite energy absorbing subfloor concepts. The shear panel at FS220 was replaced with a corrugated web energy absorber developed by the German DLR and the Australian ACS-CRC and fabricated of graphite fabric material. The shear panel at FS254 was replaced with the sinusoid energy absorber and the shear panel at FS268 was replaced with the conusoid energy absorber. Unlike the barrel section test, the original floor in the CH-46E was not replaced with polycarbonate material. However, for viewing of the subfloor response during the crash test, rectangular-shaped windows were cut into the floor panels at discrete locations and polycarbonate was used to fill these openings. Photographs of the installed conusoid and sinusoid energy absorbers taken looking through the clear polycarbonate covering are shown in Figures 19(a) and (b), respectively. The energy absorbers were 63-in. wide, 9.2-in. tall, and 1.5-in. deep and weighted approximately 2-kg. each. In comparison, the aluminum shear panels that were removed weighed 2.6-kg.

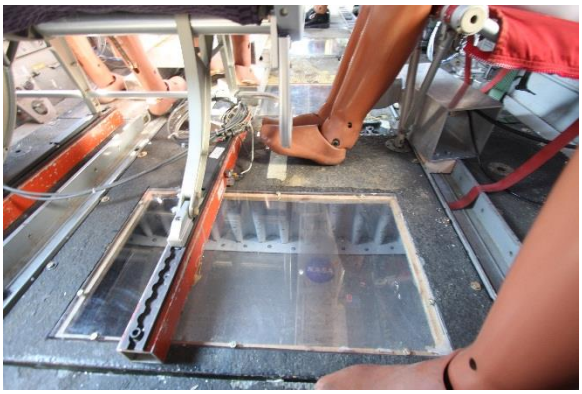

(a) Conusoid energy absorber

(b) Sinusoid energy absorber

Figure 19. Two energy absorbers as installed in TRACT 2 test article.

On October 1, 2014, the TRACT 2 full-scale crash test was conducted at the LandIR facility. A post-test photograph is shown in Figure 20. Nine organizations, including NASA, NAVAIR, DLR/ACS-CRC, FAA, US Army Aeromedical Research Laboratory (USAARL), US Army CARGO, Cobham Life Support/BAE Systems, and Safe Inc., took part in the TRACT 2 activity, contributing 18 experiments related to occupant seating and restraints, composite crashworthiness, and emergency locator transponder survivability, as described in References 3 and 19-22. The TRACT 2 test article was instrumented with over 360 data channels, including 13 ATDs, 12 on-board high-speed cameras, 10 on-board high definition cameras, and 12 external high-speed cameras. Data were recovered from over 95% of the channels. Measured impact conditions were 403.8-in/s (33.65-ft/s) forward velocity and 304.32-in/s (25.36-ft/s) vertical velocity. The airframe attitude at impact was 2.6° pitch (nose up) and 3.6° roll (left side down), and 2.5° yaw (nose right) . The total weight of the test article was 10,534-lb. The impact surface, as with TRACT 1, was a sand/clay mixture.

Figure 20. Post-test photograph of the TRACT 2 full-scale crash test.

During the impact, the outer belly skin buckled and tore between FS220 and FS286 as it plowed through the soil. The bottom skin skidded approximately 51-in. along the surface of the soil, leaving an 8- to 9-in.-deep divot (maximum depth). As the outer belly skin failed, the floor continued to move forward, which produced shearing in the subfloor beams. The outer skin was torn in several places, while the composite energy absorbing subfloor beams rotated globally under shear loading without significant crushing, as shown in the photograph of Figure 21. The severe outer skin deformation and failure is attributed to wet soil conditions, measured to have a variable moisture content. The crash test was performed days following a rainstorm. Even though the soil was covered during the storm, water was able to penetrate a seam in the tarp. The moist soil produced a higher than anticipated coefficient of friction. For example, TRACT 1 was tested under the same impact conditions onto the same soil and had a slide out of approximately 96-inch [2].

Figure 21. Post-test photograph of outer skin deformation between FS220 and FS286

TRACT 2 Finite Element Model

Development of a finite element model of the TRACT 2 test article was completed and predictions of structural impact responses were generated. The airframe model is shown in Figure 22. The model consists of: 218,251 nodes; 13,178 beam elements; 102,413 Belytschko-Tsay shell elements; 119,632 solid elements; 473 parts; 27 material properties; 34 element masses; 19 constrained nodal rigid bodies; 1 initial velocity card; and 1 body load representing gravity. The composite shell elements forming the conusoid and the face sheets of the sinusoid foam sandwich energy absorbers were represented using Mat 58, with properties listed in Table 1 with previously described techniques developed for the component level models. Finite element models of the sinusoid and conusoid energy absorbers were incorporated into the TRACT 2 model, as shown in Figure 22(b). These subfloors were located at FS254 and FS286, respectively. Nominal shell element edge length for the conusoid was 0.3-in., compared with a 0.25-in. element edge length for the sinusoid.

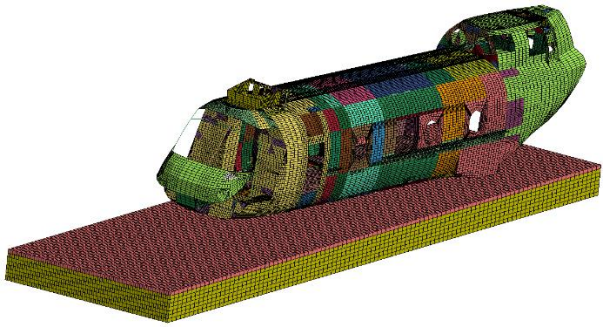

(a) Overall finite element model

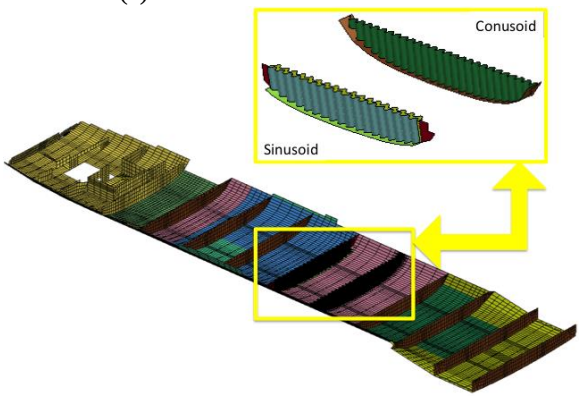

(b) Sinusoid and Conusoid models

Figure 22. Depiction of the TRACT 2 finite element model with floor energy absorbers highlighted.

The soil was represented using solid elements that were assigned Mat 5 (*MAT_SOIL_AND_FOAM) in LS-DYNA®, which is a material model for representing soil and foam [23]. The soil block was 24-in. deep x 148-in. wide x 600-in. long, as shown in Figure 22(a). A coefficient of friction of 0.5 between the airframe and the soil was used in an automatic single surface contact definition. Initially, the soil was represented as a single block with one material model assigned; however, based on the soil characterization results, the model was changed to a layered soil configuration. The top 3-in.-deep layer of soil was represented using Mat 5 with input properties obtained from soil tests conducted on gantry unwashed soil, which were performed for NASA's Orion program [24]. The bottom 21-in. deep layer was also represented using Mat 5 with input properties of soft sand, whose bearing strength matched in-situ test results conducted prior to and after the TRACT 2 crash test. The bottom and side nodes of the soil model were constrained from motion using a SPC definition in LS-DYNA®.

All nodes forming the helicopter airframe were assigned measured initial conditions of 403.8-in/s (33.65-ft/s) forward and 304.32-in/s (25.36-ft/s) vertical velocities. In addition, the TRACT 2 model was oriented to match the measured impact attitude. Seat/occupant and discrete masses, which includes the ballast mass over the sinusoid were represented using Constrained Nodal Rigid Bodies (CNRBs).

Experimental and predicted inertial properties of the TRACT 2 airframe are listed in Table 2. In general, the properties of the model compare well with test data. The crash simulation was executed using LS-DYNA® Version 971 R6.1.1 SMP (double precision) for 0.1-s, which required 74 hours and 35 minutes of CPU on a Linux-based workstation computer with 8 processors.

Table 2. Comparison of model and test weight and balance data.

	Test	Model
Weight, lb.	10,534	10,534
CG_x, in.	262.8	269.6
CG_y, in.	±0.5	-0.91
CG_z, in.	-10.0	-9.56

Nodal output was requested at locations corresponding to accelerometers mounted on the cabin floor in the test article. The locations of floor-mounted accelerometers, which were attached at the frame/floor junctions on both the left and right sides of the airframe, are illustrated in Figure 23. Test-analysis comparisons were generated at these locations and the experimental and predicted responses were filtered using a 4-pole Butterworth low-pass filter with a cutoff frequency of 60-Hz. Nodal output was also requested on floor centerline locations at FS220, FS254 and FS286, which were the locations of the retrofit energy absorbing concepts.

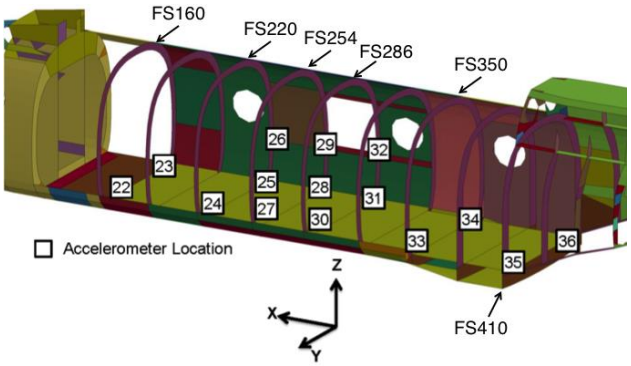

Figure 23 Schematic of fuselage section showing floor-mounted accelerometer locations.

TRACT 2 Test-Analysis Comparisons

Acceleration comparisons from locations over the composite energy absorbers along with test-analysis comparison from a subset of other locations within the airframe are presented. Both are presented to assess the validity of the overall finite element model, along with assessing the comparisons between the two retrofit energy absorbers. The first location examined was the rearmost frame section, FS410. It was at this location that the test article impacted the soil first. Figure 24 shows both forward (a) and vertical (b) accelerations.

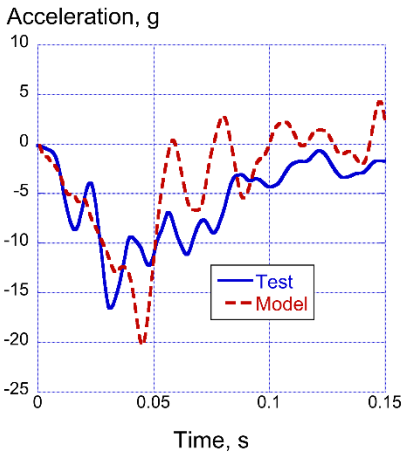

(a) Forward acceleration

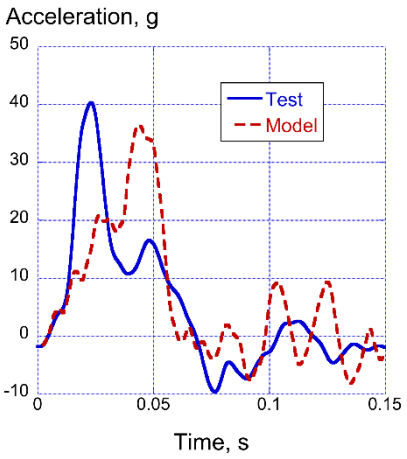

(b) Vertical acceleration

Figure 24. Forward and Vertical accelerations for FS410

In general, the finite element model agrees with the test data. In the forward direction, slight variations in the peak accelerations are seen, however the general shape and onset rate match. One major difference is the onset rate of the vertical acceleration between the test and the model. The test shows a peak acceleration of approximately 40-g occurring around 25-msec. after impact, while the model shows a slightly lower peak approximately 45-msec. after the impact. However the duration of acceleration is approximately the same.

The accelerations at FS254 were next examined. Figure 25 shows the accelerations on the existing frame section, on the left side of the test article.

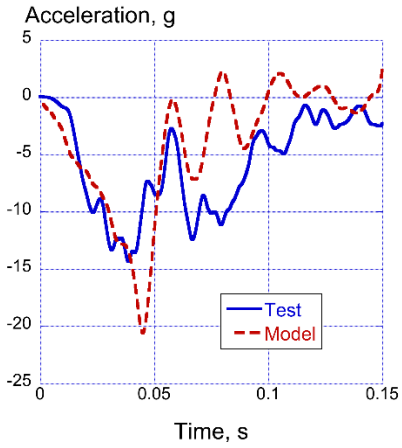

(a) Forward acceleration

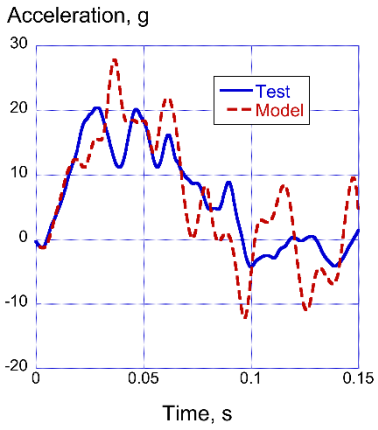

(b) Vertical acceleration

Figure 25. Forward and Vertical accelerations for FS254, left side frame

The accelerations on the left side of the test article agree in duration for both the forward and vertical directions. The forward acceleration peak of 20-g is slightly higher in the model than the test, with the post-peak response reaching 0-g at a quicker rate. The

vertical accelerations, match well both in peak values and in duration.

Next, example experimental and analytical response comparisons are shown in Figure 26 for the accelerometers mounted at the base of the double seat located directly over the conusoid at FS286, near the center of the floor. The experimental and analytical forward acceleration responses are similar and they match the duration and magnitude of the results previously documented in Figures 24 and 25 for the floor/frame intersection regions. However, the vertical acceleration results vary considerably. The experimental trace exhibits a dramatic initial peak of 60-g, which is higher than previously shown vertical acceleration traces, followed by a drop in acceleration and a subsequent peak of 22-g. The response is indicative of a sudden shock experienced by the accelerometer, as might be caused by fracture of the sides of the conusoid energy absorber from the fuselage frame at FS286. In contrast, the predicted response exhibits a stable, fairly uniform acceleration of low magnitude (approximately 20-g). This difference is due to how the test article behaved from the floor shear causing large rotations of the composite energy absorbers compared to the model behavior, which showed a stable crushing pattern.

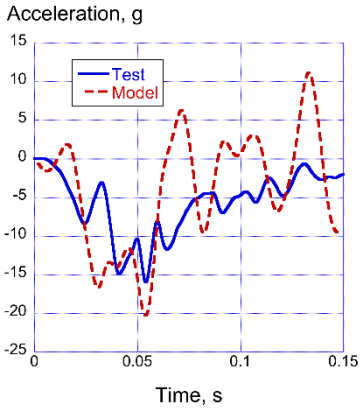

(a) Forward acceleration

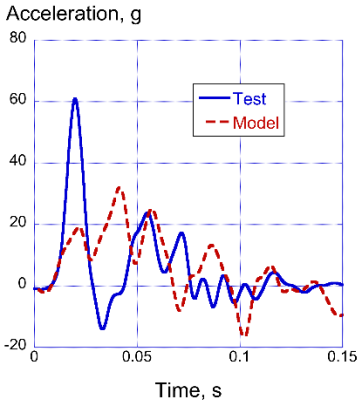

(b) Vertical acceleration

Figure 26. Forward and Vertical accelerations for conusoid energy absorber

Following the impact test, the composite subfloors were removed from the test article. Photographs of the conusoid and the sinusoid energy absorbers are shown in Figures 27 and 28, respectively. Note that both photographs show the energy absorbers as they would be positioned facing rearward. The rearward side of both energy absorbers was painted and marked for camera viewing and motion tracking. The conusoid exhibited fracturing on the left and right sides where the energy absorber attached to the fuselage frames. No evidence of crushing or plastic deformation was observed. In the model, the composite subfloor beams behaved in an ideal fashion and exhibited stable crushing. The conusoid subfloor crushed 48.8% of its original 9.2-in. height, with maximum crushing occurring at 0.06-s. The model deformation shown as a deformation overlay fringe plot, is depicted in Figure 27(b).

(a) Post-test configuration of the conusoid

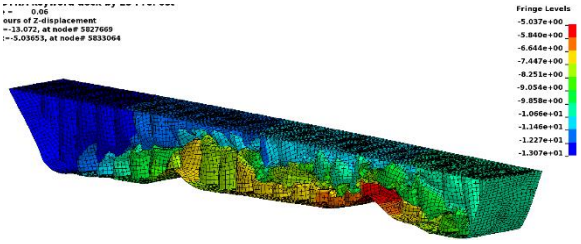

(b) Crush deformation of the conusoid simulation

Figure 27. Post-test and simulation results for the conusoid

The sinusoid displayed areas of crush initiation, especially on the bottom left side, as highlighted in the inset photograph of Figure 28(a). Note that a 600-lb. mass was attached to the floor on the left side that straddled the sinusoid energy absorber at FS254. However, the amount of crushing was estimated to be less than 0.5-in. The sinusoid subfloor crushed 42.6% of its original height with maximum crush displacement occurring at 0.06-s, which is shown in Figure 28 (b).

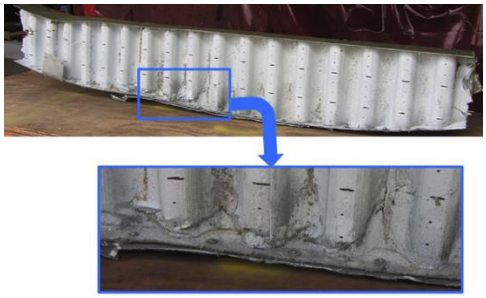

(a) Post-test configuration of the sinusoid

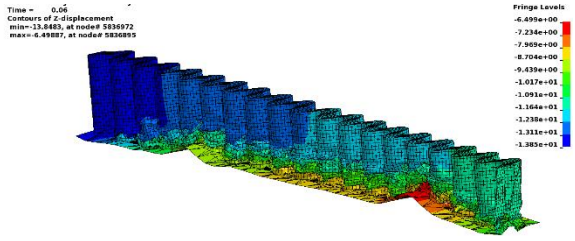

(b) Crush deformation of the sinusoid simulation

Figure 28. Post-test and simulation results for the sinusoid

CONCLUSION

Two primary objectives of this research were to design and assess the capabilities of two novel composite energy absorbers under dynamic impact loading, both via a test series using a building-block approach, but also through a series of computer simulations.

The first concept, designated the "conusoid," is a conusoidal-shaped design based on alternating right-side-up and up-side down half-cones placed in a repeating pattern. The conusoid combines a simple cone design, with sinusoidal beam geometry to create a structure that utilizes the advantages of both configurations. The conusoid was fabricated of four layers of hybrid graphite-Kevlar® fabric with layers oriented at [+45°/-45°/-45°/+45°]. The second energy absorber, designated the "sinusoid," is a sinusoidal foam sandwich design, which consists of two face sheets oriented at [±45°] fabricated of hybrid graphite-Kevlar® fabric material with a 1.5-in. closed-cell foam core separating the face sheets. The design goals for the energy absorbers were to achieve between 25- to 40-g average crush accelerations, to minimize peak crush loads, and to generate relatively long crush stroke limits under dynamic loading conditions, typical of those experienced during the TRACT 1 full-scale crash test.

The energy absorbing concepts were evaluated using a multi-level, building-block approach, including both testing and LS-DYNA® simulations. Initially, component specimens were subjected to vertical impact using a 14-ft. drop tower. The components had nominal dimensions of 12-in. in length, 7.5-in. to 9-in. height. The component tests were used to assess the energy absorption capabilities of various iterations of the two composite designs. The impact condition for all of the dynamically crushed specimens was approximately 264-in/s (22-ft/s).

After a best design was chosen from the component tests, subfloor beams of the conusoid and sinusoid configurations were manufactured and retrofitted into a barrel section of a CH-46E helicopter airframe. A vertical drop test of the barrel section was conducted at 297.6-in/s (24.8-ft/s) onto concrete. The objectives of the test were to evaluate: (1) the performance of the two energy absorbers during a full-scale drop test prior to the TRACT 2 test, (2) the fabrication methods for the energy absorbers, (3) the structural integrity of the retrofit, (4) the strength of the polycarbonate floor, and (5) imaging techniques used during the test

After successfully demonstrating that the energy absorbing designs were able to limit the transmitted loads by crushing and folding from the vertical drop test, the two energy absorbers were retrofitted into the subfloor of the TRACT 2 test article. A full-scale crash test was performed onto soil with impact conditions of 403.8-in/s (33.65-ft/s) forward and 304.32-in/s (25.36-ft/s) vertical velocity. The test article contained numerous onboard experiments; however, a major goal of the test was to evaluate the performance of novel composite energy absorbing subfloor designs for improved crashworthiness.

Major findings of this research effort are listed, as follows:

- Both the conusoid and sinusoid foam sandwich concepts proved to be excellent energy absorbers, as demonstrated through component impact tests. The conusoid exhibited stable folding and crushing up to 38.7% stroke with an average acceleration of 28.0-g, thus meeting the stated design goal. Likewise, the sinusoid absorbed energy through localized uniform folding of the face sheets and foam crushing. An average acceleration of 21.8-g was recorded for the sinusoid over 50% crush stroke.
- For both components, the LS-DYNA® predictions showed excellent comparison with test data. The LS-DYNA® model of the conusoid predicted an average acceleration of 28.4-g for the conusoid. Likewise, the average acceleration of the predicted response for the sinusoid component is 22.9-g.
- The barrel section drop test results were complicated by the fact that the conusoid energy absorber bottomed out, allowing the floor to impact the outer skin. In addition, two long bolts used to attach the concentrated mass to the floor over the sinusoid were untrimmed, allowing the bolts to impact the outer skin and deform plastically. Both of these events resulted in large increases in the acceleration responses near the end of the pulses, as measured on the two concentrated masses located over the conusoid and sinusoid energy absorbers. Despite these complications, average accelerations of 15- and 14.2-g were measured on the 681-lb and 320-lb concentrated masses located over the conusoid and the sinusoid energy absorbers, respectively.
- During the barrel section impact, the conusoid energy absorber exhibited 58% crush stroke and displayed fracturing and delamination of the hybrid composite walls. The sinusoid energy absorber exhibited 49.3% crush stroke and displayed crushing of the foam core, and fracturing of the face sheets starting from the bottom, curved edge.
- LS-DYNA® model predictions for the barrel section drop test were reasonable; however, results indicated that the model was generally too stiff. For example, the predicted maximum crush displacement of the conusoid energy absorber was 7.8-in. and the experimental maximum crush displacement was 8.67-in., a difference of approximately 0.9-in. Likewise, the predicted maximum crush displacement of the sinusoid was 5.24-in. and the experimental maximum crush displacement was 6.3-in., a difference of 1-in.
- Results from the TRACT 2 full-scale crash test were also complicated by anomalies. Moist soil increased the coefficient of friction and reduced the stopping distance of the test article by half, compared with the TRACT 1 test. Due to excessive damage of the outer belly skin, the composite energy absorbers failed to crush and rotated globally as they became separated from the floor and outer skin. Regardless, over 95% of 350-channels of data were collected during the impact test.
- Finally, based on soil anomalies and structural modifications made to the airframe, a true assessment of the conusoid and sinusoid behavior as a retrofit concepts could not be made.

ACKNOWLEDGEMENTS

The authors of this report gratefully acknowledge personnel from the Navy Flight Readiness Center in Cherry Point, NC for providing the TRACT 2 CH-46E airframe. In addition, Navy personnel provided a baseline NASTRAN model that was used as the baseline to generate the LS-DYNA® finite element model. We would also like to thank engineers, technicians and contractor personnel who work at the NASA Langley LandIR Facility for instrumenting and configuring the test articles, collecting test data, taking photographs and videos, and performing soil characterization testing.

REFERENCES

[1] Jackson, K.E., Fuchs, Y. T., and Kellas, S., "Overview of the NASA Subsonic Rotary Wing Aeronautics Research Program in Rotorcraft Crashworthiness," *Journal of Aerospace Engineering*, Special Issue on Ballistic Impact and Crashworthiness of Aerospace Structures, Volume 22, No. 3, July 2009, pp. 229-239.

[2] Annett M.S., Littell J.D., Jackson K.E., Bark L., DeWeese R., McEntire B.J., "Evaluation of the First Transport Rotorcraft Airframe Crash Testbed (TRACT 1) Full-Scale Crash Test," NASA Technical Memorandum, NASA/TM-2014-218543, October 2014.

[3] Annett M.S., "Evaluation of the Second Transport Rotorcraft Airframe Crash Testbed (TRACT 2) Full Scale Crash Test," Proceedings of the American Helicopter Society International Annual Forum 71, Virginia Beach, VA, May 3-5, 2015.

[4] Kindervater C., Thomson R., Johnson A., David M., Joosten M., Mikulik Z., Mulcahy L., Veldman S., Gunnion A., Jackson A., and Dutton S., "Validation of Crashworthiness Simulation and Design Methods by Testing of a Scaled Composite Helicopter Frame Section," Proceedings of the American Helicopter Society 67th Annual Forum, Virginia Beach, VA, May 3-5, 2011.

[5] Billac T., David M., Battley M., Allen T., Thomson R., Kindervater C., Das R., "Validation of Numerical Methods for Multi-terrain Impact Simulations of a Crashworthy Composite Helicopter Subfloor," Proceedings of the American Helicopter Society 70th Annual Forum, Montreal, Quebec, Canada, May 20-22, 2014.

[6] Littell J. D., "The Development of a Conical Composite Energy Absorber for use in the Attenuation of Crash/Impact Loads," Proceedings of the American Society for Composites 29th Technical Conference, 16th US-Japan Conference on Composite Materials, September 8-10, University of California San Diego, La Jolla, CA.

[7] Hallquist J. Q., "LS-DYNA Keyword User's Manual," Volume I, Version 971, Livermore Software Technology Company, Livermore, CA, August 2006.

[8] Hallquist J. Q., "LS-DYNA Keyword User's Manual," Volume II Material Models, Version 971, Livermore Software Technology Company, Livermore, CA, August 2006.

[9] Price J. N., and Hull D., "Axial Crushing of Glass Fibre-Polyester Composite Cones," *Composites Science and Technology*, Volume 28, 1987.

[10] Feraboli P., et al. "Design and certification of a composite thin-walled structure for energy absorption," *International Journal of Vehicle Design*, Vol. 44, Nos. 3/4, 2007.

[11] Gupta N. K. and Velmurugan, R., "Axial Compression of Empty and Foam Filled Composite Conical Shells," *Journal of Composite Materials*, Vol. 33, No. 6, 1999.

[12] Fleming D. C., and Vizzini A. J., "Tapered Geometries for Improved Crashworthiness Under Side Loads," *Journal of the American Helicopter Society*, Vol. 38, 1993.

[13] Cronkhite J.D., and Berry V.L., "Crashworthy Airframe Design Concepts, Fabrication and Testing," NASA Contractor Report 3603, NASA Contract NAS1-14890, September 1982.

[14] Farley G.L., "Crash Energy Absorbing Composite Sub-Floor Structure," AIAA Paper 86-0944, Proceedings of the 27th AIAA/ASME/ASCE/and AHS Structures, Structural Dynamics, and Materials Conference, San Antonio, TX, May 19-21, 1986.

[15] Hanagud S., Craig J.I., Sriram P., and Zhou W., "Energy Absorption Behavior of Graphite Epoxy Composite Sine Webs," *Journal of Composite Materials*, Vol. 23, No. 5, 1989, pp. 448-459.

[16] Carden H. D., and Kellas S., "Composite Energy-Absorbing Structure for Aircraft Subfloors," proceedings of the DOD/NASA/FAA Conference, South Caroline, Nov. 1993.

[17] Feraboli P., "Development of a Corrugated Test Specimen for Composite Materials Energy Absorption," *Journal of Composite Materials*, Vol. 42, No. 3, 2008, pp. 229-256.

[18] Matzenmiller A., Lubliner J., and Taylor R. L., "A Constitutive Model for Anisotropic Damage in Fiber Composites," *Mechanica of Materials*, Vol. 20, 1995, pp. 125-152.

[19] Bark L.W., "Performance Evaluation of Crash-Recording Technologies in a Full-Scale CH-46 Airframe Crash Test," Proceedings of the 71st Annual Forum of the American Helicopter Society, International, Virginia Beach, VA, May 3-5, 2015.

[20] Bark L.W., "Testing Mobile Aircrew Restraint Systems in a Full-°©-Scale CH-°©-46 Airframe Crash Test – Exploring the Limits," Proceedings of the 71st Annual Forum of the American Helicopter Society, International, Virginia Beach, VA, May 3-5, 2015.

[21] Desjardins S.P., and Labun L.C., Selectable Profile Energy Absorber System for Rotorcraft Troop Seats,"

Proceedings of the 71st Annual Forum of the American Helicopter Society, International, Virginia Beach, VA, May 3-5, 2015.

[22] Little E.J., Bakis C.E., Bark L.W., Miller S.W., Yukish M.A., and Smith E.C., "Laboratory and Field Evaluations of Up-Scaled Textile Energy Absorbers for Crashworthy Cargo Restraints," Proceedings of the 71st Annual Forum of the American Helicopter Society, International, Virginia Beach, VA, May 3-5, 2015.

[23] Fasanella E.L., Lyle K.H., Jackson K.E., "Developing Soil Models for Dynamic Impact Simulations," Proceedings of the American Helicopter Society 65th Annual Forum, Grapevine, TX, May 27-29, 2009.

[24] Thomas M.A., Chitty D.E., Gildea M.L., and T'Kindt C.M., "Constitutive Soil Properties for Unwashed Sand and Kennedy Space Center," NASA/Contractor Report, NASA/CR-2008-215334, July 2008.